Biomedical Physics & Engineering Express

PAPER

Antiproliferative effect of MoS_2 in human prostate cancer cell lines

RECEIVED
29 July 2019

REVISED
22 October 2019

ACCEPTED FOR PUBLICATION
28 October 2019

PUBLISHED
6 November 2019

Nahid Askari[1,4] **and Mohammad Bagher Askari**[2,3,4]

[1] Research Department of Biotechnology, Institute of Sciences and High Technology and Environmental Sciences, Graduate University of Advanced Technology, Kerman, Iran
[2] Department of Physics, Faculty of Science, University of Guilan, PO Box 41335-1914, Rasht, Iran
[3] Department of Physics, Payame Noor University (PNU), PO Box:19395-3697, Tehran, Iran
[4] Author to whom any correspondence should be addressed.

E-mail: n.askari@kgut.ac.ir **and** mbaskari@PhD.guilan.ac.ir

Keywords: MoS_2, LNCaP, PC3, MTT assay, real-time, western blot

Abstract

In this investigation, the anti-proliferative activity of a novel molybdenum complex was distinguished on LNCaP (as an androgen-dependent), PC3 (as an androgen-independent) cancer cells, and normal PBD2-fib cells (as a control) using MTT assay, flow cytometry, RT-qPCR, and western blotting. The MoS_2 was prepared by the hydrothermal method, and the synthetic MoS_2 characterized using XRD, EDX, FESEM, HRTEM, and Raman spectroscopies to confirm the success of the synthesis and the unique crystal structure. The cells were treated with different concentrations of MoS_2 (0, 5, 10, 20, 35 and 50 $\mu g\ ml^{-1}$) for 24, 48 and 72 h. The obtained results showed that the IC50 values for LNCaP ($21.02 \pm 0.09\ \mu g\ ml^{-1}$) and PC3 ($23.03 \pm 0.07\ \mu g\ ml^{-1}$) were significantly lower than that recorded for normal fibroblast cells ($41.56 \pm 0.012\ \mu g\ ml^{-1}$). Flow cytometry findings demonstrated that the complex is effective in reducing cancer cell viability via apoptosis. RT-qPCR data showed a decrease in *BCL2* expression and increases in *BAX* and *P53* gene expression, which were also correlated with the synthetic complex response. The expression of P53 protein increased in LNCaP and PC3 cells after treating with MoS_2. Also, these data show the anti-tumor properties of synthetic molybdenum complexes in prostate cancer cells. To conclude, the results indicated that the novel design of nanoparticles can be created a new generation of nano-therapeutics strategies in different types of cancer.

Introduction

Prostate cancer (PC) is a remarkably prevailing disease which is the second leading cause of cancer mortality [1]. Although, age is the most important factor in PC there it is also increased in those with a family history [2].

To the best of author's knowledge, androgen is essential for the survival and proliferation of prostate cells and its receptor has a critical role in prostate cancer development and progression. Androgen deprivation therapy is an effective way to treat prostate cancer, although, after 2-3 years, hormone-independent prostate cancer (HIPC) is likely to develop. The survival for both androgen-dependent and androgen-independent patients is not long (less than 20 months) [3]. Accordingly, it is necessary to provide a new therapeutic approach to treat prostate cancer to expand patients' lives.

It has been supposed that steroid hormone makes changes in the function and morphology of the target cells [4]. Therefore, it is necessary to study the basic mechanism of steroid receptor for understanding the molecular pathology of prostate carcinoma and some of other hormonally responsive neoplasms.

Even though it has been presumed for many years, that steroid-induced change affects the morphology and functional activities of the target cells, but, an exact mechanism still remains a major goal.

However, cell death through androgen receptor may use as an effective treatment in prostate cancer.

Regulation cell death by the apoptosis process plays a crucial role in cancer treatment [5]. Different proteins and gene families have been identified that are involved in stimulating the apoptosis process through intrinsic and extrinsic pathways. Among them, p53 is the inducer of apoptosis as the tumor suppressor. P53 is a positive regulator of BAX gene

expression which can be inhibited the cell cycle or induced the apoptosis in response to DNA damage in the testis [6]. The internal pathway is controlled by BAX and BCL2 genes, which are the members of the bcl2 family

Sirett *et al*, 1982 investigated that in hyperplastic prostatic tissue sodium molybdate affected the response of binding proteins to the androgens [7]. On the other hand, Duan *et al* 2015 showed that sulfur suppressed the prostate cancer cells proliferation *in vivo* [8]. Today, nanoparticles are synthetic or natural particles with 1to100 nm size. Since nanoparticles are an effective material both in terms of treatment and diagnosis of many diseases, including different kinds of cancers, most researches are concentrated on the invention of new drugs, which are essential to expansion, the therapeutic effectiveness of nanoparticles. Today, there are many approaches to Nanomedicine in cancer therapy. Recent studies demonstrated that Nanoparticles may be used for treating different disorders. Because of their size, they can cross the cell membrane and pass through the blood-brain barrier (BBB) [9].

During recent years, using new methods in the synthesis of nanoparticles is a desirable approach in nanotechnology. There are different methods to make Nanoparticles in a desirable function, shape and, size [10]. Synthesized Nanoparticles and nanotechnology is an emerging wonder in medicine, which had amazing results in the treatment of tumors. In order to assess the potential uses of Nanoparticles and different nanomedical approaches, a review of the literature is required. Numerous Nanoparticles and their performance in Nanomedicine for the treatment of cancers have been studied previously. Additionally, new trends in the synthesis of metal nanoparticles with reference to the treatment of tumors have been elaborated. In recent years, Molybdenum disulfide was used to assess its anti-tumor properties. Scientists explored the promising anti-cancer effects of various forms of synthetic MoS_2 [11–13]. Based on the recent advances; authors hope that using nanotechnology will lead to highly effective strategies for the treatment of prostate cancer in the future [14].

Among various metal nanoparticles, in this study, a synthetic nano-complex of molybdenum was used. The synthetic nanomaterials have different physicochemical properties because of their large surfaces to volume ratio. It is related to the size, shape, stabilizing and the degree of aggregation of each ligand [15].

In this study, it was determined the role and regulatory effects of androgen receptor inactivation on the death process of LNCaP cancer cell line. Also, it was tested the effect of the synthetic MoS_2 on PC3 cancer cell line to test the composite on the death of a prostate cell line as an androgen-independent cell.

Materials and methods

Synthesis and characterization of MoS_2

At first, 2 mM molybdate and 10 mmol thioacetamide were added to 30 ml deionized water. After dissolving, it was syringed into an autoclave reactor and put in the 240 °C oven at for 24 h. Then, let it cool at room temperature overnight [16]. Methanol and water were used to wash the final product which was arid in the 40 °C oven for 24 h after centrifuging. The resulted product was a black powder of MoS_2.

The morphology and size of MoS_2 were evaluated using scanning electron microscopy (ESEM; TESCAN MIRA3-XMU) and Transmission electron microscopy (TEM; Philips CM30). X-ray diffraction (XRD, PW1800 Philips) was taken to further investigate the MoS_2. The structure of the synthetic MoS_2 was also evaluated using Raman, energy dispersive x-ray (EDX) spectroscopies (Hitachi SU3500).

Cell lines and cultures

LNCaP, PC3 and human dental fibroblast (PBD2-fib) cells as a normal cell, were obtained from the National Cell Bank of Pasteur Institute, Tehran, Iran. Cells were cultured in RPMI 1640 in a 5% CO_2 humidified incubator at 37 °C. The media supplemented with 10% (v/v) fetal bovine serum, penicillin (100 U/ml), streptomycin (100 μg ml^{-1}), and amphotericin B (1 μg ml^{-1}). The culture medium was renewed every 2 days and cells were subcultured at 80% cell confluence.

3-[4, 5-dimethylthiazole-2-yl]-2, 5-diphenyltetrazolium bromide (MTT) assay

In order to study the cytotoxicity of the synthetic MoS_2, cells were plated in triplicate at the density of 5×10^3 per well in a 96-microplate well for the MTT assay. The experiment was containing negative and positive controls. Cells were treated with the different concentration of synthetic MoS_2 (0 5, 10, 20, 35, 50 μg ml^{-1}).

Cell viability was produced by the reduction of MTT to formazan. MTT was diluted in PBS and added to the culture in the final concentration of 0.5 mg ml^{-1}. It was followed by 3 h incubation at 37 °C, then its medium was removed and 100 μl DMSO was added to each well, and the absorbance values were determined by Eliza reader at 570 nm with a microplate reader (BIO-TEK INSTRUMENTS, USA).

Finally, the percentage of viable cells was calculated according to the following formula:

The survival rate of cells (%) = (absorbance of experimental group/ absorbance of the blank control group) × 100.

Additionally, Molybdenum complexes were solved in methanol a solution, which is not a common

Table 1. The sequence and product size of the primers used in the study.

Primer	Tm	Primer sequence	Product size (bp)
β- actin	64	F: GGACATCCGCAAAGACCTGTA R: ACATCTGCTGGAAGGTGGACA	189
Bcl2	61	F: GTGGATGACTGAGTACCTGA R: AGCCAGGAGAAATCAAACAGA	119
Bax	61	F: TTTGCTTCAGGGTTTCATCC R: CAGCTCCATGTTACTGTCCA	154
P53	60	F: AACGGTACTCCGCCACC R: CGTGTCACCGTCGTGGA	94

solvent for cell cultures. Therefore, to check the cytotoxic effect of methanol, it was used to treat the cells.

Flow cytometry detection of the cells

The amount of apoptosis was determined by annexin-V staining and propidium iodide (PI) was used for detection of necrotic cells. Cells were treated with media containing different concentrations of MoS_2 (0–50 $\mu g\,ml^{-1}$) for 24 h. Treated Cells were detached and stained with PE-Annexin V and PI in the dark at room temperature, according to the manufacturer's protocol of Annexin V apoptosis detection kit I (BD Pharmingen™, USA). Then, the stained cells analyzed by flow cytometry (Partec, Germany).

RT-qPCR

Total RNA was extracted from the LNCaP, PC3 cancer cells and normal PBD2-fib cells using RNX-plus TM Reagent (Cinnaclon, Iran) according to the manufacturer's protocol before and after treatment. Then cDNA was synthesized from 1 μg of total RNA using M-MuLV-RT and random hexamer primers (Thermo Fisher Scientific Inc.) in a final volume of 20 μl. Each reaction was accompanied by two negative controls without template RNA and M-MuLV-RT enzyme. RT-qPCR was reached using the primer sequences listed in table 1. The selected primers were amplified using SYBR Green Takara Master Kit according to the instructions of the supplier on Rotor-Gene 3000 (Corbett Research, Australia). The initial concentration of each sample was normalized against the β-actin. Temperature conditions were as follows: 95 °C for 30 s, 45 cycles of 95 °C for 5 s, 60 °C–62 °C (depending on primers) for 30 s and 72 °C for 30 s analysis of the gene expression completed using the comparative cycle threshold method ($2^{-\Delta\Delta Ct}$ method) [17]. The paired two-sample t-test (Excel, Microsoft Office 2010, USA) was applied to evaluate the mean of the gene expression and the significance was reported at $p < 0.05$.

Western blotting

LNCaP and PC3 cells were subjected to MoS_2 (35 $\mu g\,ml^{-1}$) for 24 h. Next, the total protein was extracted by TNE buffer (Tris-HCl 'pH = 7.8'(10 mM), 0.1% Na-deoxycholate, 1% NP-40, 150 mM NaCl, EDTA (1 mM), 1 mg ml^{-1} each of leupeptin, aprotinin and pepstatin, 1 mM PMSF, 1 mM NaF and 1 mM Na_3VO_4). The samples were cooled by putting them on ice and their proteases were inhibited using protease inhibitor (Roche, Switzerland). They were electrophoresed on a 12% SDS-PAGE and then shifted to the nitrocellulose membrane at 4 °C. Then, the membrane was covered with blocking solution (TBST and 5% fat-free dry milk) at room temperature for about 25 min which TBST buffer contained 200 mM NaCl, 50 mM Tris and 0.1% Tween-20 (pH = 7.4). Then it was hybridized with P53 antibody (1: 500, Santa Cruz Biotechnology, Inc.) for about 12 h at 4 °C. After that the incubation of the membrane was done using the HRP-Goat anti-mouse IgG antibody (1: 1000, Santa Cruz Biotechnology, Inc.) after washing 3 times by using TBST solution. Then, chemiluminescence reagent (Santa Cruz Biotechnology, Inc.) was added and eventually to Kodak x-ray film was used for detection Western blots protein bands.

Statistical analysis

The statistical analysis was performed with SPSS Version 20. Analysis of variance (ANOVA) and Duncan's multiple range test (DMRT) was accomplished at the 0.05 level.

Results and discussion

MoS_2 characterization

Atoms in each crystal structure illustrate a specific direction of scattering x-rays; XRD is used to evaluate the crystalline construction of the sample in which a 3D pattern of electrons' density can get by measuring the scattering angle and intensity. Based on this density, that can be achieved the atomic position, chemical bonds, and other related information.

XRD analysis was used to evaluate the crystalline structure, crystallite planes and phase composition of synthetic MoS_2. Four peaks at 14.3, 33.3, 39.6, and 58.4° in addition to a weaker peak at 49.8° were observed indicating a multi-crystalline construction of

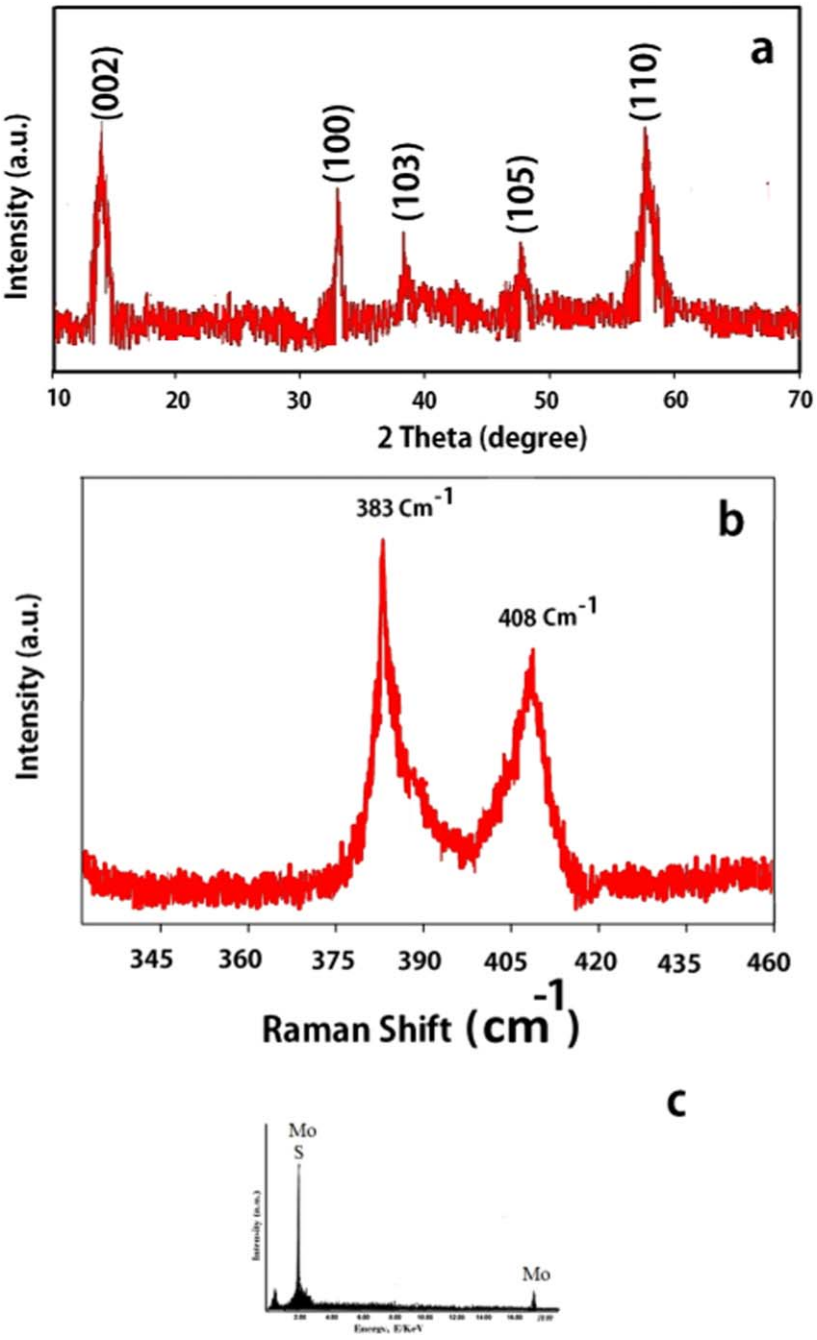

Figure 1. XRD spectrum of MoS_2 (a), Raman spectrum of MoS_2 (b) and EDX analysis of MoS_2 (c).

MoS_2. It also declared the high purity and hexagonal structure of the synthetic specimen (figure 1(a)).

The Raman spectroscopy of MoS_2 showed 2 strong bands in the 200–500 cm^{-1} region, which were, 383 and 408 cm^{-1} declared the hexagonal structure (figure 1(b)).

The EDX spectrum results and the existence of 2 peaks defined to molybdenum and sulfur confirmed that the synthesis method was done correctly (figure 1(c)).

The SEM was used to check the surface morphology of MoS_2 particles (figure 2(a)). The FESEM put electrons to have images which they show the higher resolution of the sample's surface containing higher levels of magnification and penetration depth. It can be taken in comparison to optical microscopes facilitating microstructural investigations and specimens' surface studies. The deliberated sample has a tough surface with pores which are connected with some channels related to these holes. These examinations affirm the formation of MoS_2. The HRTEM showed microstructure properties of MoS_2 (figure 2(b)). Dark fringes are vacant spaces between the fringes and MoS_2 tending to be a network which is related to MoS_2 layers.

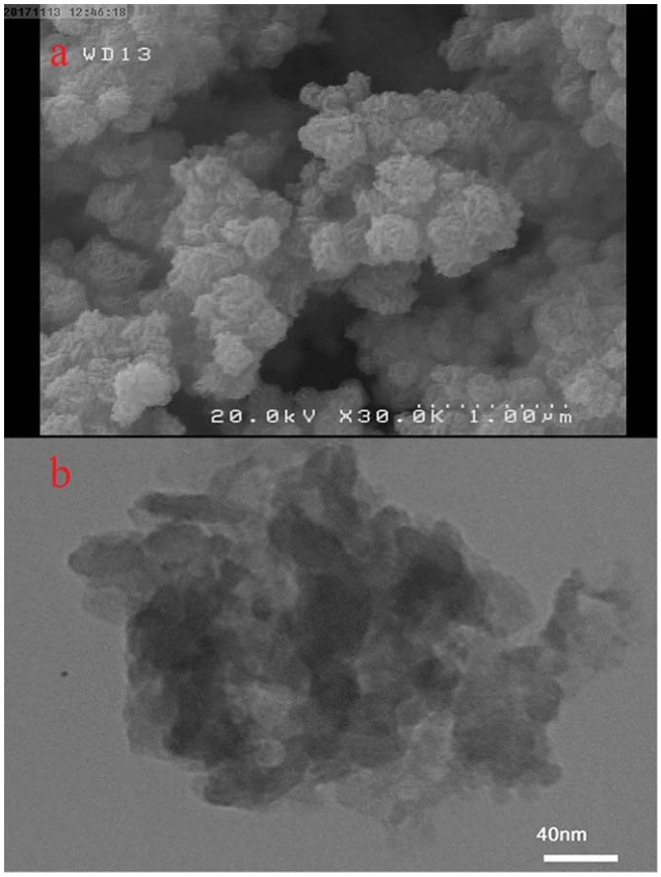

Figure 2. FESEM micrograph of MoS_2 (a) and HRTEM image of MoS_2 (b).

MTT assay

The results from the MTT assay revealed that methanol has low toxicity with few or no necrotic cells.

The cytotoxic activity of MoS_2 for LNCaP, PC3 cells was studied using the MTT assay. The cells were treated with various concentrations of synthetic MoS_2. The results demonstrated that MoS_2 had inhibitory effects on the proliferation of prostate cancer cells. At 20 μg and 35 μg, MoS_2 affected the cells and decreased the growth of them by 80%. On the other hand, the strong inhibiting effect of MoS_2 on LNCaP, PC3 prostate cancer cells were all evident 50 $\mu g\,ml^{-1}$ but it was also had an influence on the PBD2-fib. Interestingly, MoS_2 at the range of 0to 35 μg were affected insignificantly at all doses on the PBD2-fib cells (figure 3).

Then, the IC_{50} value which was related to the concentrations that suppress the proliferation by 50% relative to the control, estimated using the SPSS version 13.0 statistical analysis software.

As represented in figure 4, the concentration for causing 50% cell death or IC50 value was $41.56 \pm 0.012\ \mu g\,ml^{-1}$ in the normal cells treated with MoS_2. On the other hand, it was made the same effect (50% cell death) at a very low concentration of 21.02 ± 0.09 and 23.03 ± 0.07 for LNCaP and PC3 cells respectively. It was confirmed lower cytotoxicity of MoS_2 on the normal cell line.

Flow cytometry analysis

The effect of MoS_2 on cells was distinguished using flow cytometry. After MoS_2 treatment, flow cytometry results showed that MoS_2 inhibited the proliferation of LNCaP and PC3 cells by promoting apoptotic death (figure 5). The histograms of flow cytometric analysis showed the rate of apoptosis and necrosis using annexin-V-FITC and PI.

RT-qPCR

The qualities of the extracted RNAs were studied using spectrophotometry and an OD ratio of A260/A280 for RNA was achieved, which will be approximately equal to 1.8–2 in optimal conditions. RT-qPCR results of treated cells using Mos_2 showed the down-regulation of *BCL2* ($p < 0/.05$). *P*53 and *BAX* gene showed overexpression compared to the control ($p < 0.05$) and with decreasing expression of *BCL2*, the *BCL2/BAX* ratio also increased. This was pertinent to the apoptosis which is related to changes of mitochondrial permeabilization and function.

Western blotting

The Western blot results illustrated the p53 protein expression in treated LNCaP and PC3 cells in comparison to the control group (figure 6(a)). The quantification of the bands was done using densitometry after

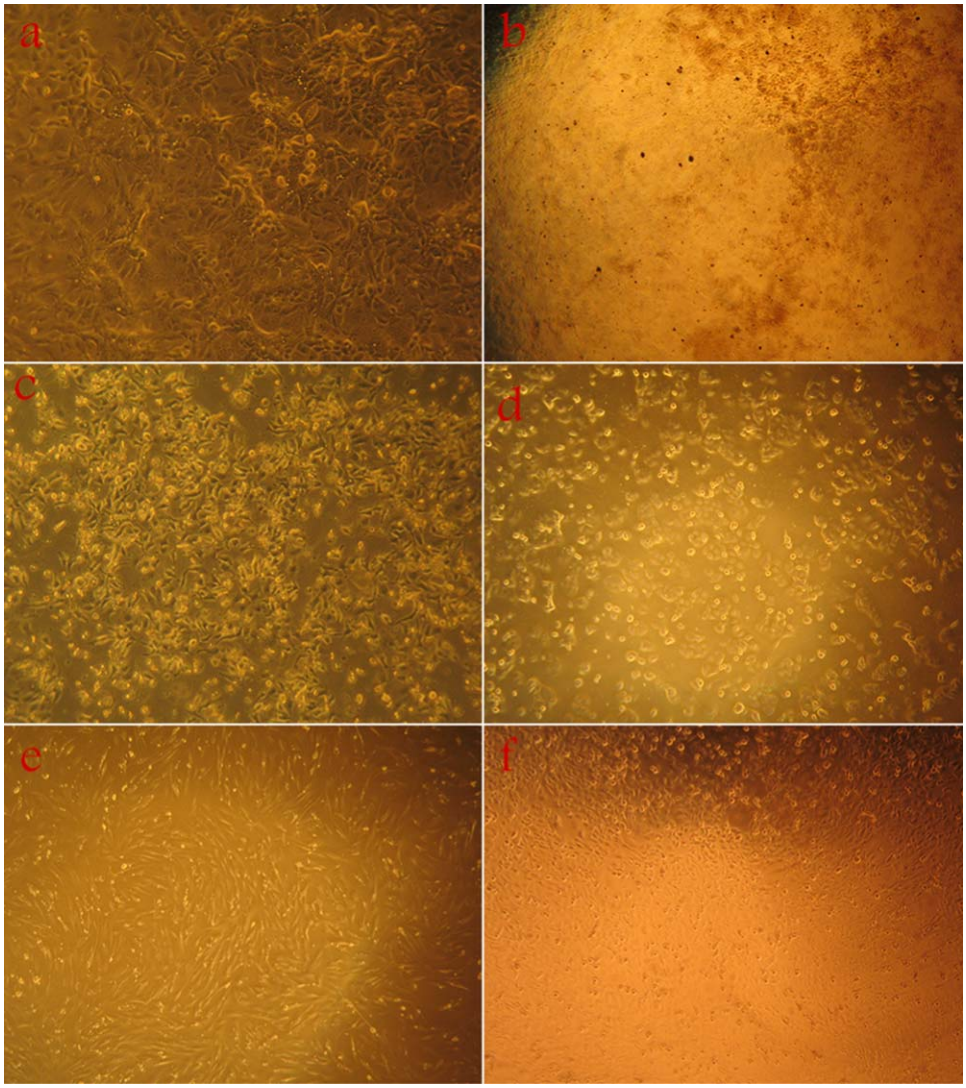

Figure 3. Results from MTT assay test using PC3 cell line before treating by MoS_2 (a), after 24 h (b), LNCaP cell line before treating by MoS_2 (c), after 24 h (d), PBD2-fib cell line before treating by MoS_2 (e), after 24 h (f).

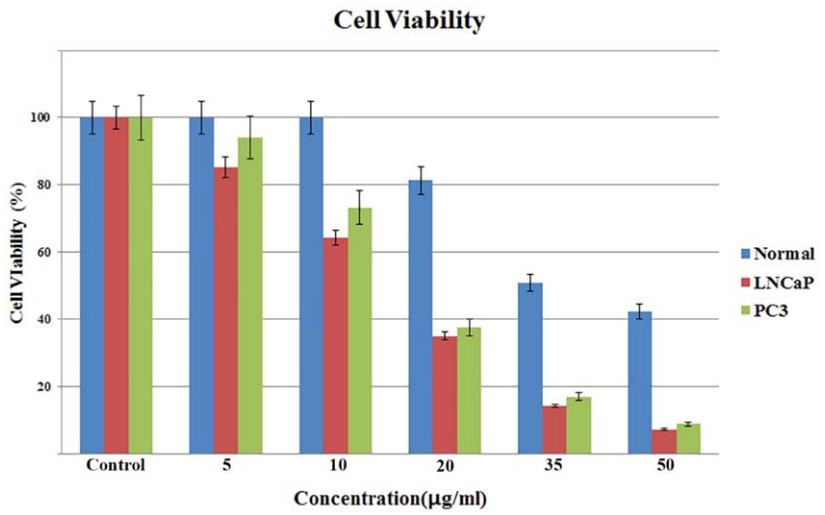

Figure 4. Effect of Mos_2 on cell viability (%) of LNCaP, PC3, and PBD2-fib cell lines determined by MTT assay. Each value is represented as mean ± SD of triplicate experiments.

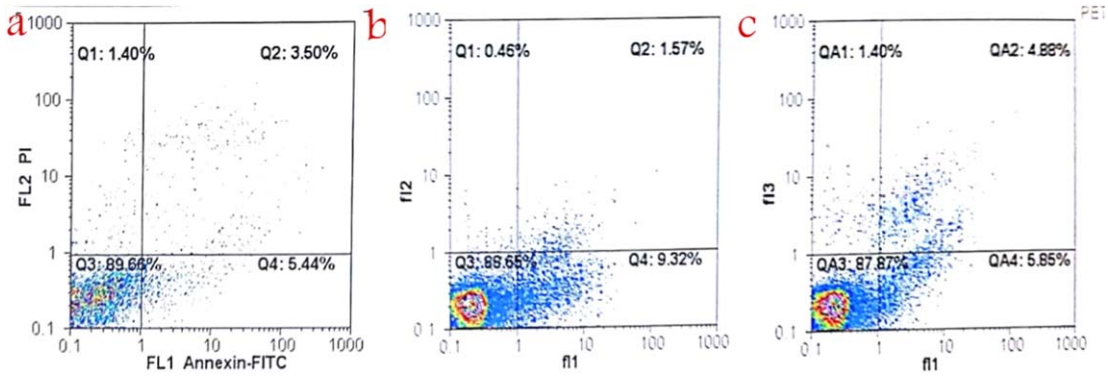

Figure 5. MoS_2 induces apoptosis in prostate cancer cells. Prostate cancer cells were treated without or with indicated compounds for 24 h. Cell apoptosis was noticed using flow cytometry with annexin-V-FITC and PI. Q1, Q2, Q3 and Q4 parts of the flow cytometry histogram show necrosis cells, the late apoptosis cells, normal cells, and the early apoptosis cells respectively in fibroblast (a), PC3 (b) and LNCaP (c) cells.

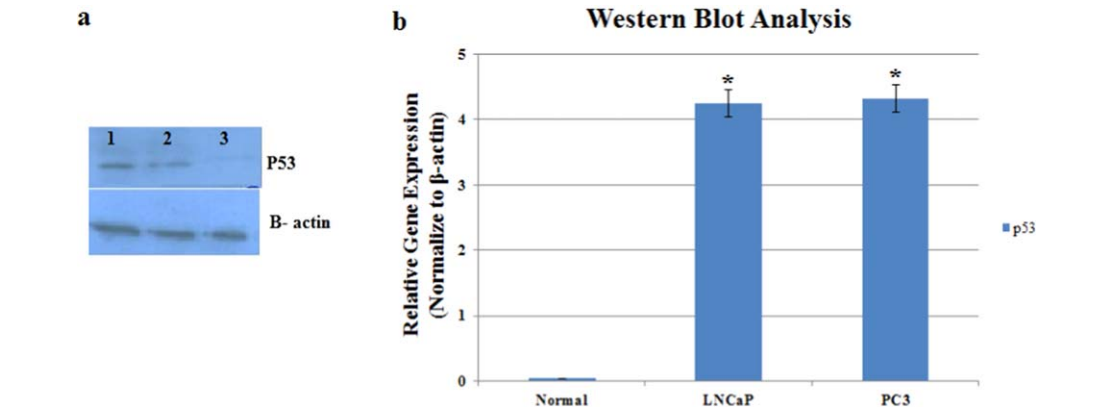

Figure 6. (a) P53 protein Western blot results of LNCaP and PC3 cells (1 and 2) and the control group (3). (b) The bands of Western blot were quantified using densitometry after normalization to the protein expression of β-actin. Data are means $\pm$ SD of triplicate experiments. $^{*}p < 0.05$.

normalizing to β-actin. Data are means $\pm$ SD of three experiments ($p < 0.05$) (figure 6(b)).

Prosthetic tissue in normal condition consists of the basal cells, neuroendocrine (NE) cells and luminal epithelial cells. Most of the prostate cancers are classified as adenocarcinomas. In adenocarcinomas, malignant cells grow in an uncontrolled manner but luminal epithelial cells establish glandular formation in addition to androgen receptor [18].

Therefore, androgen deprivation therapy also called androgen suppression therapy is used for the remedy in prostate cancer which can block the production and use of androgen in addition to induced apoptosis in cancer cells is androgen-dependent manner. Unfortunately, this treatment causes androgen-independent cancer cells to maintain and continue activity in the absence of androgen. On the other hand, in the early stages of diagnosis of prostate cancer based on histopathology methods, only uncontrolled cell proliferation in the prostate tissue is exploring and the exact type of cancer is not mentioned.

Accordingly, it is necessary to use a treatment method for eradicating all types of prostate cancer cells (both in androgen-dependent and androgen-independent manner).

Molybdenum is a transition element and forms the active site of Molybdenum enzymes which are an essential part of the carbon, nitrogen and sulfur cycles. Molybdenum cofactors synthesized by a conserved pathway that consists of four steps in cells [19]. On the other hand, the most important role of Sulfur in cells is its role in oxidative stress which suggests the effect of Sulfur compounds in basic functions as the homeostasis of chemical cell structure and detoxifying mechanisms. Since molybdenum plays an essential role in the sulfur cycle, it needs to make complex by a special cofactor in order to get catalytic activity inside the cells [20]. In this regard, Ubiquitin and ubiquitin-like proteins are signaling messengers which control cellular functions, like apoptosis, the proliferation of the cells, and the repair of DNA. It is proposed that Ubiquitin protein modification evolved from prokaryotic sulfur transfer systems. Molybdenum cofactor and thiamin are sulfur-containing cofactors whose biosynthesis includes an important sulfur transfer step which uses unique sulfur carrier proteins [21].

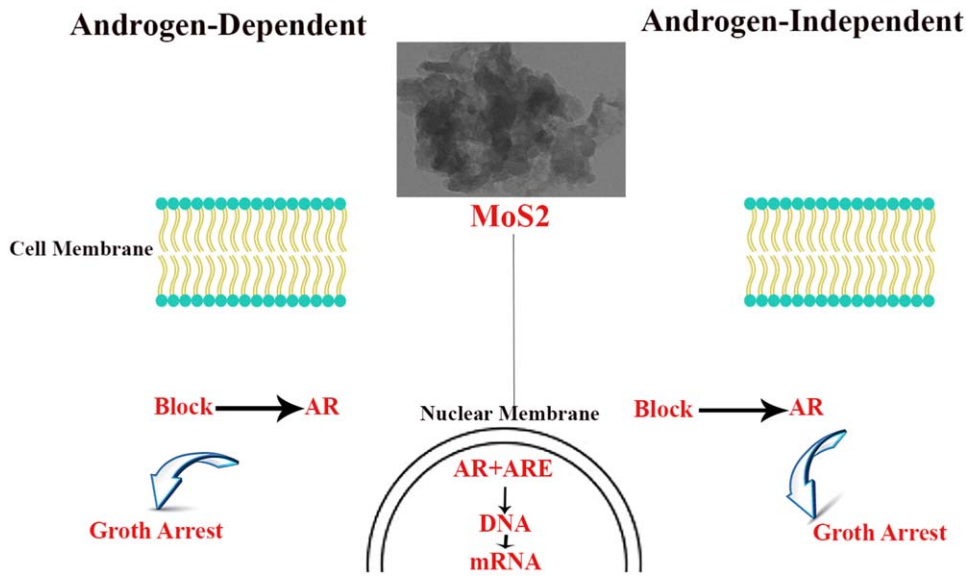

Figure 7 - Androgen signaling blocked through using MoS_2 in prostate cancer cells. Abbreviations: AR, androgen receptor; ARE, androgen response element; mRNA, messenger RNA.

Therefore, MoS_2 probably was degraded inside the cells to use in the specific mechanisms.

Different experimental methods have used extremely to treat prostate cancer. Recently, Synthetic nanoparticles have a vast area of research through their uses in a wide variety of areas in medicine like cancer therapy and drug delivery [12]. In this regard, LNCaP and PC3 Cell lines were the dominant experimental prostate cancer models for years. Generally, LNCaP and PC3 have been worth to study prostate cancer because they possess significantly different characteristics. LNCaP cells express luminal differentiation markers as androgen receptor but PC3 cells don't. For this reason, LNCaP cells are androgen-dependent, and thus androgen withdrawals inhibit their proliferation. While PC3 cells proliferate normally in androgen-deprived media because they are androgen-independent cells.

Recently, apoptosis-inducing drugs have been introduced to treat cancer. Therefore, it is crucial to evaluate the balance between the increase and decrease of tumor cells. Because it is possible that inhibits the growth of cancer by limiting the tumor cell growth [22].

Since in this study, the efficacy of synthetic MoS_2 was evaluated in prostate cancer cells.

As mentioned, this synthetic material with the presence of molybdenum and sulfur was able to inhibit the growth of prostate cancerous cells (both in androgen-dependent and androgen-independent manners).

The response of MoS_2 treatment towards LNCaP and PC3 cells were further respected by conducting MTT assay, flow cytometry, and RT-qPCR. It was provided a scheme illustrating the possible suppression mechanisms of MoS_2 nanoparticles on the proliferation of prostate cancer cells by blocking androgen receptors activation in the cytoplasm and inhibited them to pass through the nuclear membrane and bind to the androgen receptors elements to promote transcription (figure 7).

According to the results of this study, MoS_2 had significantly high effects on the proliferation of both LNCaP and PC3 cancer cells. The results of the RT-qPCR and western blot illustrated that the gene (*P53*, *BAX*, and *BCL2)* and protein (P53) expression in the treated groups were different in comparison to the control. The P53protein expression in LNCaP and PC3 cells were higher than the control. Moreover, using MoS_2 changed the expression levels of *BAX* and *BCL*-2 in LNCaP and PC3 cells and induced a significant down-regulation of BAX gene in LNCaP and PC3 cell lines after 24 h and 48 h of exposure in comparison to PBD2-fib cells. Whereas, study the P53 protein by Western Blot demonstrated a statistically significant, in both LNCaP and PC3 cells inducing by MoS_2. Altogether, it can result that MoS_2 can affect prostate cancer cells even in gene and protein expression levels.

The results surprisingly showed that even the small amount of MoS_2 is efficient to make changes in prostate cancer cells proliferation such that apoptosis was induced.

However, apoptosis is a highly regulated process that plays a crucial role in homeostasis. It has been demonstrated that control by various intracellular and extracellular factors.

The p53 is located at 17pl3 which is changed in human cancers. It is a transcription factor expressed at low levels under normal conditions, but its expression is increased upon DNA damage, oncogene activation, nutritional deprivation, and hypoxia. P53 is one of the most-studied genes, which is involved in the

formation and/or progression of cancer. Oncogenic functions of P53 are often observed in tumor proliferation, invasion and even drug resistance [23].

On the other hand, BCL-2 is an anti-apoptotic factor and BAX is a pro-apoptotic factor. The overexpression of *BCL-2* has been associated with chemotherapy resistance in various human cancers, and preclinical studies showed that factors targeting anti-apoptotic *BCL-2* activity are necessary for the treatment of cancer. For this reason and to investigate the effect of the MoS_2 on the induction of cell death in prostate cancer cells, the expression level of *BCL2* and *BAX* gene were determined after treatment. The results demonstrated that the expression of *BCL2* is significantly decreased ($p < 0.05$). It was also evident that expression of *BAX* and *P53* increased ($p < 0.05$). The balance between BAX and *BCL2* involves activating the apoptosis through the mitochondrial pathway. Changing the *BCL2/BAX* ratio in this study can confirm the activation of the apoptosis pathway in cancer cell lines that were treated by MoS_2 [24].

On the other hand, apoptosis is a highly regulated process that plays a very important role in maintaining homeostasis in multi-cellular organisms. Apoptosis has been shown to be controlled by many intracellular and extracellular factors. BCL-2 is an anti-apoptotic factor and BAX is a pro-apoptotic factor, which can prevent apoptosis by blocking the release of cytochrome-c from the mitochondria. The overexpression of BCL-2 has been related to the chemotherapy resistance in various human cancers, and preclinical researches have demonstrated that factors targeting anti-apoptotic BCL-2 activity are crucial in the treatment of cancer [25]. For this reason and to find the effect of the MoS_2 on the induction of cell death in cancer cells, the expression level of BCL2 and BAX gene were measured after cell treatment. The results showed that the expression of BCL2 is significantly decreased ($p<0.05$). It was also evident that expression of BAX increased ($p < 0.05$). The balance between BAX and BCL2 through the regulation of the mitochondrial membrane integrity involves activating the mitochondrial pathway of apoptosis. Increasing the BAX/BCL2 ratio in this study can confirm the activation of the apoptosis pathway in cancer cell lines that were treated by extract [26].

Evidence that receptors in many tissues are stabilized by sodium molybdate, thus, Sirett *et al* 1982, studied the effect of the molybdate which is related to the receptor levels with response to endocrine therapy in prostatic cancer. They demonstrated that 10 mmol l^{-1} molybdate caused a threefold rise in androgen binding affinity in the cytosol and small progress in the number of progestin-binding sites in the cytosol [7].

LNCaP and PC3 cells have been illustrated the apoptosis after MoS_2 treatment. Since it was examined whether the MoS_2 caused the reduction in cell viability which was evaluated with the MTT assay. Thus reducing the number of living cells could be related to the apoptosis induction in prostate cancer cells.

Study the cytotoxicity of MoS_2 on the samples in the present study demonstrated that direct dose-response relationship, in that cell viability reduced at higher concentrations (figure 4). Such a pattern was established in the human normal cell line in which the cytotoxic effect of MoS_2 nanoparticle was recognized on PBD2-fib. But the mortality rate of normal cells was much lower than cancer cells.

Therefore, synthesized MoS_2 Nanoparticle represented higher cytotoxicity in prostate cancer cells than the normal cells. These results were in accordance with the findings of Gao *et al* 2018 which indicate that MoS_2 -PEG nanospheres had an effective role in the destruction of tumors [27]. However, our results revealed that mentioned MoS_2 Nanoparticles were less toxic on the normal cell line of PBD2-fib. The toxicity of MoS_2 Nanoparticles have been also illustrated in the previous studies [28–30]. On the other hand, Zhao *et al* 2018 synthesized a nanoparticle of high dispersive mesoporous silica/MoS_2-PEG which was showed efficient drug loading and photothermal performance. The *in vitro* and *in vivo* results demonstrated that it could be used for cancer treatment [31]. On the other hand, Wang *et al* 2017 demonstrated that colloidal stable and biocompatible WS_2-PVP nanosheets could be used to treat tumors [32]. However, comparing the measured IC50 for MoS_2 revealed that these particles at nano size which were more toxic for prostate cancer cell line than normal cells.

On the other hand, study the cytotoxic activity of the synthesized MoS_2 was demonstrated that IC50 in LNCaP and PC3 cell lines were lower than PBD2-fib cells. In this study, MoS_2 strongly inhibited the prostate cancer cell lines proliferation by using MTT assay. MoS_2 promoted the apoptosis through the apoptotic pathway in cancer cells by altering the expression of *BAX* and *BCL2* genes which were checked using RT-qPCR measurements. The balance between BAX and BCL2 through the regulation of the mitochondrial membrane integrity involves activating the mitochondrial pathway of apoptosis.

Leanddas Nurdiwijayanto *et al* (2017) demonstrated that atmospheric environment has an important role in the stability and quality of synthesized MoS_2. They reported that it was related to the reoxidation process of MoS_2, whereas the MoS_2 lose their residual negative charge-inducing its lateral fracture and aggregation. Therefore our synthesized MoS_2 could be used to treat the cells [33]. It was demonstrated that chemically exfoliated MoS_2 stand the aggregation and lateral fracture upon long storage in ambient air, which was related to the reoxidation of MoS_2. Because the stability and quality of chemically laminated MoS_2 were related to the reoxidation procedure. According to previous studies, in this research, it is reported a strategy to improve the effective delivery of a Nano agent for prostate cancer therapy through selectively

both androgen-dependent and androgen-independent manner. Our results are in agreement with those reported by Yang (2018) in that it was demonstrated that MoS_2 Nanoparticles could be used for combined tumor photothermal and chemotherapy [12]. But here it was showed that MoS_2 nanoparticles can be used effectively in prostate cancer based on its own properties in attaching and penetrating prostate cancer cells. However, since scientists have shown that MoS_2 can carry anti-cancer drugs, it can be used in combination with some common prostate chemotherapy drugs, because in this way it will have more beneficial synergistic effects in the treatment of cancer cells. Whether it can be concluded that MoS_2 nanoparticle would find application in cancer therapy and pharmacology. Moreover, Liu *et al* 2017 showed that MoS_2 @Fe-ICG/Pt nanocomposites had bioimaging properties in addition to its antitumor effects; therefore, it can be used in photodynamic cancer for cancer diagnosis and treatment [11].

In the present study, the combined treatment of using both sulfur and molybdenum reduced cell proliferation both in androgen-dependent and androgen-independent prostate cancer cells. Because the most important problem in prostate cancer is androgen-independent cases which were resistant to the most typical prostate cancer drug as an androgen-deprivation therapy [34]. It is necessary for the development of new therapeutic strategies for chemotherapy-resistant cancer cell investigations.

Finally, the considerable antiproliferative effect of MoS_2 on prostate cancer cells indicates the possibility to use the mixture of sulfur and molybdenum in anticancer therapies. Our results indicate the advantages of the ability of MoS_2 to reduce the proliferation of cell growth in prostate cancer. MoS_2 eventuate as possible recourse to current therapeutic approaches which are toxic in noncancerous tissues. Our findings demonstrated that MoS_2 might increase prostate cancer cell death via apoptosis. MoS_2 may illustrate a novel therapeutic approach for prostate cancer.

Conclusion

In conclusion, our data demonstrated that MoS_2 showed anticancer effects against LNCaP and PC3 prostate cancer cell lines *in vitro*.

The mechanism may induce apoptosis via a mitochondrial pathway based on the changes in the expression of *BCL2, BAX* and therefore cause the death of cells. Finally, the present study suggests that MoS_2 may have therapeutic effects on prostate cancer and could be a new candidate in this field. Actually, the molecular target of MoS_2 and its mechanism are still unknown, and the author has plans to find it using animal models and bioinformatics methods.

Acknowledgments

This research was supported by the Graduate University of Advanced Technology, Kerman, Iran. Project number: 7/97/2704.

Conflicts of interest

The authors declare no conflicts of interest.

ORCID iDs

Mohammad Bagher Askari https://orcid.org/0000-0003-2094-6234

References

[1] Bashir M N 2015 Epidemiology of prostate cancer *Asian Pac. J. Cancer Prev.* **16** 5137–41
[2] Daniyal M, Siddiqui Z A, Akram M, Asif H M, Sultana S and Khan. A 2014 Epidemiology, etiology, diagnosis and treatment of prostate cancer *Asian Pac. J. Cancer Prev.* **15** 9575–8
[3] Raymond E *et al* 2017 An appraisal of analytical tools used in predicting clinical outcomes following radiation therapy treatment of men with prostate cancer: a systematic review *Radiation Oncology* **12** 56
[4] McCarty K S Jr and McCarty K S Sr 1977 Steroid hormone receptors in the regulation of differentiation. A review *The American Journal of Pathology* **86** 705
[5] Vazquez A, Elisabeth E B, Levine A J and Bond G L 2008 The genetics of the p53 pathway, apoptosis and cancer therapy *Nat. Rev. Drug Discovery* **7** 979
[6] Boekelheide K 2005 Mechanisms of toxic damage to spermatogenesis *JNCI Monographs* **2005** 6–8
[7] Sirett D A N and Grant J K 1982 Effect of sodium molybdate on the interaction of androgens and progestins with binding proteins in human hyperplastic prostatic tissue *J. Endocrinol.* **92** 95–10
[8] Duan F *et al* 2015 Sulfur inhibits the growth of androgen-independent prostate cancer *in vivo Oncology letters* **9** 437–41
[9] Sadowska-Bartosz I and Bartosz G 2018 Redox nanoparticles: synthesis, properties and perspectives of use for treatment of neurodegenerative diseases *Journal of Nanobiotechnology* **16** 87
[10] Singh J, Dutta T, Kim K H, Rawat M, Samddar P and Kumar P 2018 Green'synthesis of metals and their oxide nanoparticles: applications for environmental remediation *Journal of nanobiotechnology* **16** 84
[11] Liu B, Li C, Chen G, Liu B, Deng X, Wei Y and Lin J 2017 Synthesis and optimization of MoS_2@ Fe_3O_4-ICG/Pt (IV) nanoflowers for MR/IR/PA bioimaging and combined PTT/PDT/chemotherapy Triggered by 808 nm Laser *Advanced Science* **4** 1600540
[12] Yang H, Zhao J, Wu C, Ye C, Zou D and Wang S 2018 Facile synthesis of stable colloidal MoS_2 nanoparticles for combined tumor therapy *Chem. Eng. J.* (https://doi.org/10.1016/j.cej.2018.06.100)
[13] Zhao J, Xie P, Ye C, Wu C, Han W, Huang M and Chen H 2018 Outside-in synthesis of mesoporous silica/molybdenum disulfide nanoparticles for antitumor application *Chem. Eng. J.* **351** 157–68
[14] Laurent S, Forge D, Port M, Roch A, Robic C, Vander Elst L and Muller R N 2008 Magnetic iron oxide nanoparticles: synthesis, stabilization, vectorization, physicochemical characterizations, and biological applications *Chem. Rev.* **108** 2064–110
[15] Mercatelli R *et al* 2011 Quantitative measurement of scattering and extinction spectra of nanoparticles by darkfield microscopy *Appl. Phys. Lett.* **99** 131113

[16] Zhou Z *et al* 2014 Hydrothermal fabrication of porous MoS_2 and its visible light photocatalytic properties *Mater. Lett.* **131** 122–4
[17] Rao X, Huang X, Zhou Z and Lin X 2013 An improvement of the 2^(–delta delta CT) method for quantitative real-time polymerase chain reaction data analysis *Biostatistics, bioinformatics and biomathematics* **3** 71
[18] Arutyunov A S *et al* 2018 Prosthodontic treatment of edentulous patients with postoperative mandibular defects of oncological origin *Stomatologiia* **97** 54–8
[19] Schwarz G 2016 Molybdenum cofactor and human disease *Curr. Opin. Chem. Biol.* **31** 179–87
[20] Marelja Z, Chowdhury M M, Dosche C, Hille C, Baumann O, Löhmannsröben H G and Leimkühler S 2013 The L-cysteine desulfurase NFS1 is localized in the cytosol where it provides the sulfur for molybdenum cofactor biosynthesis in humans *PLoS One* **8** e60869
[21] Lake M W, Wuebbens M M, Rajagopalan K V and Schindelin H 2001 Mechanism of ubiquitin activation revealed by the structure of a bacterial MoeB–MoaD complex *Nature* **414** 325
[22] Johnstone R W, Ailsa J F and Mark J S 2008 The TRAIL apoptotic pathway in cancer onset, progression and therapy *Nat. Rev. Cancer* **8** 782
[23] Yi J and Luo J 2010 SIRT1 and p53, effect on cancer, senescence and beyond *Biochimica et Biophysica Acta (BBA)-Proteins and Proteomics* **1804** 1684–9
[24] Armstrong J S 2006 The role of the mitochondrial permeability transition in cell death *Mitochondrion* **6** 225–34
[25] Papaliagkas V *et al* 2007 The proteins and the mechanisms of apoptosis: a mini-review of the fundamentals *Hippokratia* **11** 108
[26] Sogwagwa N, Davison G, Khan S and Solomon W 2016 P9. Correlation of radiation induced apoptosis with Bax and Bcl-2 protein expression *Physica Medica: European Journal of Medical Physics* **32** 163
[27] Gao S, Zhou H, Cui S and Shen H 2018 Bottom-up synthesis of MoS_2 nanospheres for photothermal treatment of tumors *Photochemical & Photobiological Sciences* **17** 1337–45
[28] Han J, Xia H, Wu Y, Kong S N, Deivasigamani A, Xu R and Kang Y 2016 Single-layer MoS_2 nanosheet grafted upconversion nanoparticles for near-infrared fluorescence imaging-guided deep tissue cancer phototherapy *Nanoscale* **8** 7861–5
[29] Li X, Gong Y, Zhou X, Jin H, Yan H, Wang S and Liu J 2016 Facile synthesis of soybean phospholipid-encapsulated MoS_2 nanosheets for efficient *in vitro* and *in vivo* photothermal regression of breast tumor *Int. J. Nanomed.* **11** 1819
[30] Wang J, Tan X, Pang X, Liu L, Tan F and Li N 2016 MoS_2 quantum dot@ polyaniline inorganic-organic nanohybrids for *in vivo* dual-modal imaging guided synergistic photothermal/radiation therapy *ACS Applied Materials & Interfaces* **8** 24331–8
[31] Zhao J, Xie P, Ye C, Wu C, Han W, Huang M and Chen H 2018 Outside-in synthesis of mesoporous silica/molybdenum disulfide nanoparticles for antitumor application *Chem. Eng. J.* **351** 157–68
[32] Wang S, Zhao J, Yang H, Wu C, Hu F, Chang H and Huang M 2017 Bottom-up synthesis of WS2 nanosheets with synchronous surface modification for imaging guided tumor regression *Acta Biomater.* **58** 442–54
[33] Nurdiwijayanto L, Ma R, Sakai N and Sasaki T 2017 Stability and nature of chemically exfoliated MoS_2 in aqueous suspensions *Inorg. Chem.* **56** 7620–3
[34] Jäntti M H, Talman V, Räsänen K, Tarvainen I, Koistinen H and Tuominen R K 2018 Anticancer activity of the protein kinase C modulator HMI-1a3 in 2D and 3D cell culture models of androgen-responsive and androgen-unresponsive prostate cancer *FEBS Open Bio* **8** 817–28